



## Fate of microplastics and mesoplastics carried by surface currents and wind waves: A numerical model approach in the Sea of Japan



Shinsuke Iwasaki<sup>a,\*</sup>, Atsuhiko Isobe<sup>a</sup>, Shin'ichiro Kako<sup>b</sup>, Keiichi Uchida<sup>c</sup>, Tadashi Tokai<sup>c</sup>

<sup>a</sup> Research Institute for Applied Mechanics, Kyushu University, 6-1 Kasuga-Koen, Kasuga 816-8580, Japan

<sup>b</sup> Graduate School of Science and Engineering, Kagoshima University, 1-21-40 Korimoto, Kagoshima 890-0065, Japan

<sup>c</sup> Tokyo University of Marine Science and Technology, 4-5-7 Konan, Minato-ku, Tokyo 108-8477, Japan

### ARTICLE INFO

**Keywords:**  
Microplastics  
Mesoplastics  
Sea of Japan  
Stokes drift  
Particle tracking model

### ABSTRACT

A numerical model was established to reproduce the oceanic transport processes of microplastics and mesoplastics in the Sea of Japan. A particle tracking model, where surface ocean currents were given by a combination of a reanalysis ocean current product and Stokes drift computed separately by a wave model, simulated particle movement. The model results corresponded with the field survey. Modeled results indicated the micro- and mesoplastics are moved northeastward by the Tsushima Current. Subsequently, Stokes drift selectively moves mesoplastics during winter toward the Japanese coast, resulting in increased contributions of mesoplastics south of 39°N. Additionally, Stokes drift also transports micro- and mesoplastics out to the sea area south of the subpolar front where the northeastward Tsushima Current carries them into the open ocean via the Tsugaru and Soya straits. Average transit time of modeled particles in the Sea of Japan is drastically reduced when including Stokes drift in the model.

### 1. Introduction

Plastic waste accounts for about 70% of marine debris. Because of exposure to ultraviolet radiation and mechanical erosion, it is gradually degraded into small plastic fragments that can be categorized by size as macroplastics (greater than a few centimeters), mesoplastics (> 5.0 mm), microplastics (< 5.0 mm), and nanoplastics (less than a few micrometers) (Gregory, 1996; Andrady, 2011; Cole et al., 2011). Small plastic fragments, called “primary microplastics” by Cole et al. (2011), are also used in the manufacturing of cosmetics and cleaning products and in air blasting (Gregory, 1996; Andrady, 2011). The term “small plastic fragments” is used hereafter to refer to all fragments smaller than mesoplastics. Of note, microplastics smaller than 1.0 mm are of similar size to food organisms such as zooplankton and thus, they might be ingested by a wide range of marine organisms (e.g., Browne et al., 2008; Boerger et al., 2010; Murray and Cowie, 2011; Cole et al., 2015; Desforges et al., 2015). Current knowledge of the ecological impact of microplastics is poor. However, the true scale of their damage might materialize in the future because they never completely disappear from the environment, and because the abundance of microplastics will increase gradually unless the discharge of plastic waste ceases.

To predict the potential influence of marine plastic pollution it is critical to elucidate the sources, fate, and accumulation zones of small plastic fragments, where the harm to marine organisms might be most severe. However, few studies on the transport processes of buoyant small plastic fragments have considered the motion in the turbid uppermost layer of the ocean. The combination of a particle tracking model (PTM) and surface ocean currents provided by ocean reanalysis products or satellite observations is inadequate for simulating the movement of small plastic fragments, although such combinations have been used widely in reproducing the oceanic transport of relatively large marine debris (e.g., Kubota, 1994; Maximenko et al., 2012; Kako et al., 2014). Difficulty arises from the fact that pelagic small plastic fragments are composed mostly of polyethylene or polypropylene, which are less dense than seawater (Isobe et al., 2014); thus, they move within the uppermost layer (depth: < 5 m) of the water column (Reisser et al., 2015). Isobe et al. (2014) suggested that small plastic fragments are carried partly by the mass transport (Stokes drift) generated in the uppermost layer in response to wind waves, as well as by ocean currents that extend into deeper layers. However, the effects of Stokes drift are not incorporated in either the ocean reanalysis products used widely by the oceanographic community (e.g., Usui et al., 2006; Chassignet et al., 2007; Miyazawa et al., 2009; Hirose et al., 2014).

\* Corresponding author.

E-mail addresses: [iwasaki@riam.kyushu-u.ac.jp](mailto:iwasaki@riam.kyushu-u.ac.jp) (S. Iwasaki), [aisobe@riam.kyushu-u.ac.jp](mailto:aisobe@riam.kyushu-u.ac.jp) (A. Isobe), [kako@oce.kagoshima-u.ac.jp](mailto:kako@oce.kagoshima-u.ac.jp) (S. Kako), [kuchida@kaiyodai.ac.jp](mailto:kuchida@kaiyodai.ac.jp) (K. Uchida), [tokai@kaiyodai.ac.jp](mailto:tokai@kaiyodai.ac.jp) (T. Tokai).

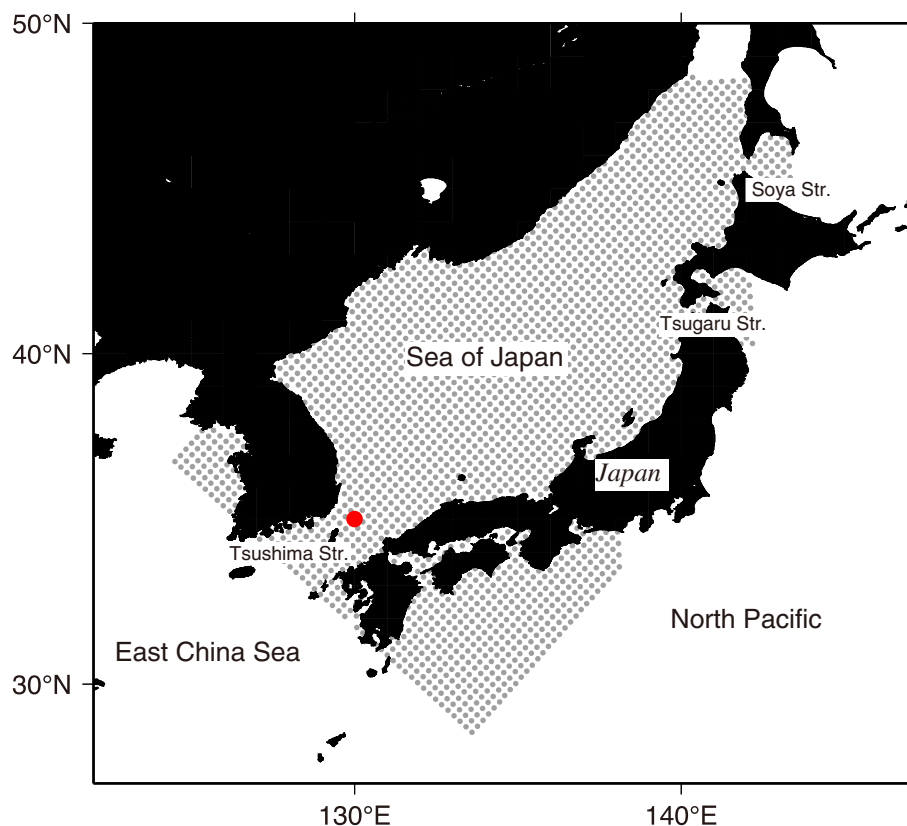


**Fig. 1.** Model domain of the PTM experiments (stippled). Red dot indicates the release position of the modeled particles in the Tsushima Strait. (For interpretation of the references to color in this figure legend, the reader is referred to the web version of this article.)

2013) or the satellite-derived ocean currents deduced by geostrophy (e.g., Bonjean and Lagerloef, 2002; Willis and Fu, 2008).

The objective of the present study was to establish a numerical model that could reproduce the transport processes of small plastic fragments in the ocean. Currently, small plastic fragments are widespread throughout the world's oceans (Cózar et al., 2014; Eriksen et al., 2014; Isobe et al., 2014; Zhao et al., 2014; Enders et al., 2015; Isobe et al., 2015; Isobe et al., 2017). In particular, the East Asian seas around Japan are regarded as a "hot spot" of microplastics because their total particle count is estimated at 1,720,000 pieces  $\text{km}^{-2}$ , which is 16 times greater than the North Pacific and 27 times greater than the average of the world's oceans (Isobe et al., 2015). Thus, the Sea of Japan (Fig. 1) was chosen as the domain for the present numerical modeling because Isobe et al. (2015) surveyed areas within this ocean, and their data were used for the model validation in this study. This study had two advantages in addressing the numerical simulation of the distribution of small plastic fragments. The first was the use of a three-dimensional PTM in which the modeled particles were carried by a combination of the surface ocean currents provided by ocean reanalysis data and the Stokes drift computed separately in a wave model driven by satellite-derived winds. In addition to marine plastic pollution research, the transport process of small plastic fragments is an interesting topic in physical oceanography because transport systems within the highly turbid uppermost layer of the ocean are poorly understood. The second advantage was that the modeled results obtained in the present study were validated using data acquired during intensive mesoplastics and microplastics field surveys around Japan in 2014 and 2015. The incorporation of Stokes drift into the PTM was justified by comparison of the observed and modeled distributions of small plastic fragments. In addition, the comparison established the limitations of the presented model in reproducing the transport behavior of small plastic fragments.

## 2. Method

### 2.1. Modeled Stokes drift and surface ocean currents

The University of Miami wave model version 1.0.1 (UMWM) (Donelan et al., 2012; <http://yyy.rsmas.miami.edu/groups/umwm/>) was used to compute the Stokes drift over the model domain ( $20^{\circ}\text{--}55^{\circ}\text{N}$ ,  $115^{\circ}\text{--}150^{\circ}\text{E}$ ) with  $0.25^{\circ}$  horizontal resolution. The UMWM resolves 37 wave frequencies from 0.0313–2.000 Hz with 32 directional bins. The wave model was driven by daily wind data acquired by the Advanced Scatterometer (ASCAT) (Kako et al., 2011; <http://mepl1.riam.kyushu-u.ac.jp/~kako/ASCAT/NetCDF/>) with  $0.25^{\circ}$  resolution in both latitude and longitude. TheETOPO1 (<http://www.ngdc.noaa.gov/mgg/global/global.html>) was used to provide the bottom topography and coastlines. The Stokes drift velocity ( $U_{St}$ ) in the UMWM is computed as follows:

$$U_{St} = \int_0^{2\pi} \int_0^{\infty} \omega k^2 \frac{\cosh[2k(d+z)]}{2\sinh^2 kd} F(k, \theta) dk d\theta, \quad (1)$$

where  $\omega$ ,  $k$ ,  $\theta$ , and  $F(k, \theta)$  are the angular frequency, wave number, wave direction measured counterclockwise from east, and wavenumber variance spectrum, respectively, all of which are computed in the UMWM. The direction of Stokes drift is identical to  $\theta$ . In addition,  $d$  and  $z$  represent the finite ocean depth and vertical position measured upward from the sea surface ( $z = 0$ ), respectively. The computation was conducted for the period January 1 through December 31, 2014. The significant wave heights and Stokes drift were both saved once daily (00:00 UTC) during the computation period. The Stokes drift was dumped at 1-m vertical intervals from depths of 0 to 5 m.

The horizontal velocities computed by the Data assimilation Research of the East Asian Marine System (DREAMS; Hirose et al., 2013) in the uppermost layer (defined as depths  $> 4$  m in Hirose et al.

(2013) were added linearly to the Stokes drift to provide the ambient surface ocean currents used for the PTM. The DREAMS mostly covers the East Asian marginal seas ( $23^{\circ}$ – $52^{\circ}$ N,  $117^{\circ}$ – $143^{\circ}$ E) with  $1/15^{\circ} \times 1/12^{\circ}$  horizontal resolution. This linear combination might be unjustified because kinetic energy transfer occurs from the winds to both ocean currents and wind waves (hence, Stokes drift) in reality, whereas ocean general circulation models driven by winds always receive the total kinetic energy transferred from the atmosphere. Thus, adding Stokes drift might introduce excessive kinetic energy into the numerical model. However, the sea surface height (hence, surface geostrophic flow) in the DREAMS product is adjusted to satellite-derived sea surface height, excluding the wind waves by spatiotemporal smoothing. See <http://dreams-i.riam.kyushu-u.ac.jp/vwp/> for a detailed description of the DREAMS product. In addition, the magnitude of wind stress is reduced by 18% according to the preliminary optimization based on climatological temperature and salinity observational data (Hirose, 2011). It is therefore likely that the kinetic energy required for generating wind waves is reduced drastically in the DREAMS product. Thereby, in the present application, it was assumed that the linear combination of Stokes drift and DREAMS currents provided reasonable surface currents for use in the PTM.

## 2.2. Particle tracking model

The PTM was established in a three-dimensional domain extending in the zonal ( $x$ ), meridional ( $y$ ), and vertical ( $z$ ) directions. The model domain, covering the entire Sea of Japan (see Fig. 1), was divided into  $1/12^{\circ}$  grid cells in both latitude and longitude, and it was located within both the UMWM and the DREAMS domains. In the PTM, the modeled particles move within a layer between the depths of 0–5 m. This is because small plastic fragments are assumed to drift within the uppermost layer (depth: < 5 m), as shown in Reisser et al. (2015). In the present application, the modeled particles were prevented from being washed ashore onto the modeled land. As adopted in Kako et al. (2014), when a modeled particle moved to a land cell, it was returned to the cell in which it was located at the previous computational time step. Different from Kako et al. (2014), however, the drag force exerted directly by winds (i.e., leeway drift; Richardson, 1997) was not included in the PTM because the small plastic fragments were considered to move entirely beneath the sea surface.

Horizontal positions [ $\mathbf{X} = (x, y)$ ] at time  $t + \Delta t$ , where  $\Delta t$  (= 360 s) represents the time increment of the PTM, were computed as:

$$\mathbf{X}(t + \Delta t) = \mathbf{X}(t) + \mathbf{U}\Delta t + \frac{1}{2} \left( \mathbf{U} \cdot \nabla_H \mathbf{U} + \frac{\partial \mathbf{U}}{\partial t} \right) \Delta t^2 + R\sqrt{2K_h \Delta t} (\mathbf{i}, \mathbf{j}), \quad (2)$$

where  $\mathbf{U}$  [=  $(u, v)$ ],  $K_h$ ,  $\mathbf{i}$ , and  $\mathbf{j}$  are the horizontal current vector, horizontal diffusivity, and unit vectors in the zonal ( $x$ ) and meridional ( $y$ ) directions, respectively (Isobe et al., 2009). Here,  $R$  represents a random number generated at each time step with an average and standard deviation of 0.0 and 1.0, respectively; these values were determined following Proctor et al. (1994). Here, the final term on the right-hand side indicates stochastic motion. The horizontal current vectors were provided by a combination of the DREAMS product in the uppermost layer and the Stokes drift at depths of 0 and 5 m. The horizontal diffusivity in Eq. (2) was computed using the Smagorinsky scheme (Smagorinsky, 1963) with the horizontal velocities mentioned above.

The vertical positions ( $Z$ ) of the modeled particles at time  $t + \Delta t$  were solved numerically using those at time  $t$  as follows:

$$Z(t + \Delta t) = Z(t) + w(t)\Delta t. \quad (3)$$

The vertical velocity ( $w$ ) was calculated from a combination of a rise velocity based on the experimental trials of Reisser et al. (2015) and a random walk as follows:

$$w(t) = 0.002\delta + \frac{R\sqrt{2K_z \Delta t}}{\Delta t}, \quad (4)$$

where  $\delta$  is the particle size (shown below); note, the coefficient of 0.002 was used to compute the rise velocity with units of  $\text{m s}^{-1}$  using  $\delta$  in mm. Here, the final term on the right-hand side indicates stochastic motion. In the ocean, small plastic fragments are mostly made of polyethylene and polypropylene (Isobe et al., 2014; Reisser et al., 2015). Although the rise velocity of the fragments depends on the density of the polymer types, the effects of density were neglected because the density difference between the above two polymer types is relatively small (~10%; Andrady, 2011), and because the abundance of small plastic fragments collected in our field surveys was not categorized according to polymer type. The vertical diffusivity,  $K_z$ , was computed as:

$$K_z = 1.5u_*kH_s, \quad (5)$$

where  $u_*$  represents the frictional velocity of water (= 0.00012  $W_{10}$ ),  $k$  is the von Karman constant (0.4),  $H_s$  is the significant wave height, and  $W_{10}$  is the 10-m wind speed (Kukulka et al., 2012). To determine  $H_s$ , the significant wave heights computed using the UMWM were employed. In addition, ASCAT data were used to provide the 10-m wind speed. The surface currents derived from the DREAMS, Stokes drift and significant wave height computed using the UMWM, and ASCAT 10-m wind speeds were all interpolated linearly in both space and time in the PTM. When a particle moved downward into a layer deeper than 5 m, it was returned immediately to the 5-m depth because the DREAMS ocean currents in the uppermost layer (< 4 m) only were used for computational simplicity. Nonetheless, this simplification had little effect on the modeled particle motion because the abundance of particles reaching this relatively deep layer was very small (less than a few percent in relation to the top layer), as shown later in Fig. 5.

## 2.3. Experimental procedure

### 2.3.1. Three-dimensional PTM experiment

A three-dimensional PTM experiment (hereinafter referred to as the first PTM experiment) was conducted to reproduce the distributions of small plastic fragments observed in 2014 and 2015. According to Jambeck et al. (2015), mismanaged plastic waste in China and Southeast Asian countries accounts for about 60% of the global total (based on their Data S1). Thus, we assumed that small plastic fragments in the Sea of Japan would be carried from the East China Sea, which is surrounded by the above areas, via the Tsushima Strait that constitutes a unique “entrance” for ocean currents emptying into the Sea of Japan. We started the PTM experiment with the modeled Sea of Japan (Fig. 1) devoid of particles. Then, 60 modeled particles with different sizes (shown below) were released daily at 0-m depth at a single point in the Tsushima Strait ( $35^{\circ}$ N,  $130^{\circ}$ E; red dot in Fig. 1). The computation then continued to the end of year 10 when the modeled particles were distributed throughout the entire model domain by the surface currents computed using Eqs. (1)–(4). In the present application, the surface currents were based on data derived from the DREAMS and ASCAT in 2014, the first year of the surveys around Japan. The 10-year computation was conducted by repeatedly using these current and wind data only. Thus, interannual variations in the distribution of small plastic fragments were neglected in the present study because of the difficulty in detecting any such variation in the observed results.

Modeled particles with sizes of 10.0, 5.0, 3.0, 1.0, 0.5, and 0.3 mm were used in the present application; note that 0.3 mm is close to the minimum detection size in the field experiment, as shown later (Section 2.5). The particles from 0.3 to 5.0 and from 5.0 to 10.0 mm can be categorized as micro-sized and meso-sized particles, as in the conventional definition (Andrady, 2011; Cole et al., 2011). In the oceans, the numbers of small plastic fragments increase as their sizes decrease (Cózar et al., 2014; Isobe et al., 2014; Enders et al., 2015; Isobe et al.,

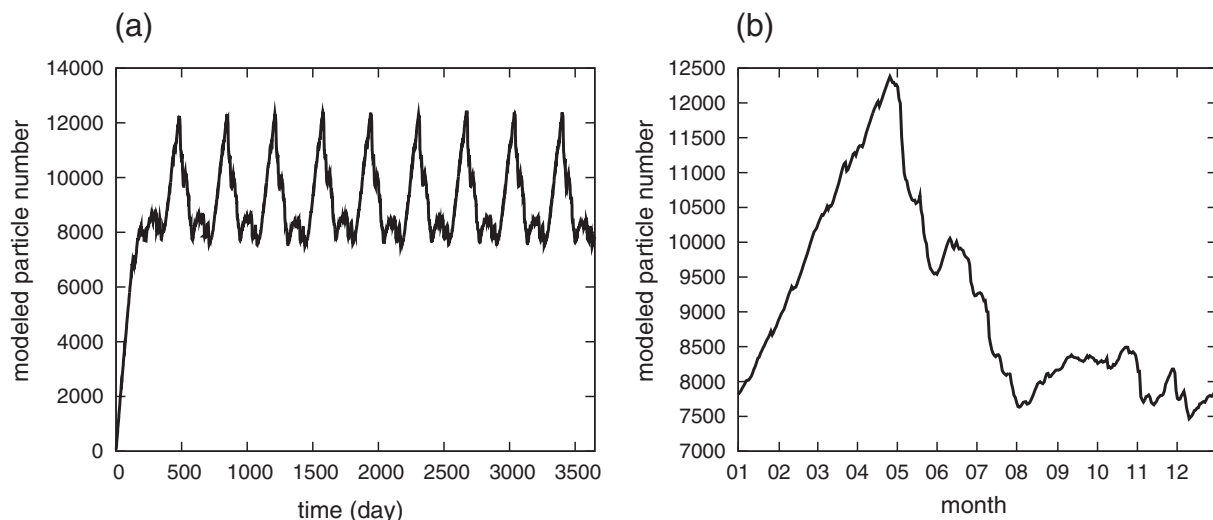


**Fig. 2.** Time series of the modeled particle numbers integrated spatially over the Sea of Japan ( $35^{\circ}$ – $45^{\circ}$ N,  $130^{\circ}$ – $140^{\circ}$ E) from the beginning of (a) year 1 and (b) year 10 to the end of year 10. Numbers of modeled particles indicate an integration of all sizes from 0.3 to 10.0 mm computed by the three-dimensional PTM (the first PTM experiment).

2015) because pieces of large marine plastic debris gradually degrade into multiple smaller pieces. Thus, the numbers of small plastic fragments actually observed in the Tsushima Strait differed depending on their size. However, in the present application, 10 modeled particles of each size (hence, 60 in total) were released uniformly in the strait once daily. This was because the objective was to reproduce the spatial distributions of particles with different sizes within the Sea of Japan (shown later in Fig. 4). In the present study (except in Fig. 4 for comparison with the observations performed using Neuston nets), the map of the particle numbers in each grid cell is based on the particle numbers integrated vertically from the depth of 0 to 5 m to reduce wind/wave influences that might have altered the vertical distribution.

### 2.3.2. Two-dimensional PTM experiment

A novel point in the present study was the incorporation of Stokes drift into the three-dimensional PTM to reproduce the behavior of the movement of the small plastic fragments. Thereby, the second PTM experiment was performed to demonstrate the advantage of incorporating Stokes drift. The PTM results obtained using surface currents provided by the DREAMS both with and without Stokes drift implemented in the surface layer (i.e., where Stokes drift is maximal) were compared. These model experiments were conducted on a two-dimensional plane extending in the zonal and meridional directions. Vertical motion was neglected in this second PTM experiment; therefore, the sizes that were used only for computing vertical velocity (Eq. (4)) were not assigned to the modeled particles. The computation period, release position, and numbers of modeled particles were all the same as in the first PTM.

### 2.4. Average transit time

The above two experiments provided average transit times (Takeoka, 1984) for particles passing through the Sea of Japan. In general, the average transit (also known as the turnover time) can be considered suitable for evaluating the time taken for water or material moving from a specific inlet to reach an outlet (Takeoka, 1984). In this application, the average transit time can be regarded as an index reflecting the environmental risk associated with small plastic fragments. This is because the chance of ingestion of the fragments by marine organisms (Browne et al., 2008; Boerger et al., 2010; Murray and Cowie, 2011; Cole et al., 2015; Desforges et al., 2015) might increase the longer the fragments remain within the Sea of Japan. The average transit time was computed in a manner such that the annually

averaged particle count integrated over the model domain was divided by the supply rate (i.e., 60 particles daily in the present case) at the inlet (Takeoka, 1984).

### 2.5. Field surveys for collecting small plastic fragments

In the present study, the modeled results were validated using the distributions of microplastics and mesoplastics observed around Japan during July–September in both 2014 and 2015; 88% of the surveys were conducted in July and early August. The results of the 2014 surveys have been published in Isobe et al. (2015); however, the results of the 2015 field surveys are included here for comparison. The procedures of net sampling and particle counting were described in Isobe et al. (2015); thus, only brief descriptions are provided in the following. The surveys were conducted using two training vessels: *T/V Umitakamaru* and *T/V Shinyomaru*, both belonging to the Tokyo University of Marine Science and Technology. Neuston nets with a flowmeter were towed by each vessel to collect the small plastic fragments drifting in the surface (approx. < 1 m) layer. The net mouth dimensions, length, and mesh size of each net were  $75 \times 75$  cm, 3 m, and 0.35 mm, respectively. Once the surveys were completed, the readings from the flowmeters installed at the mouths of the nets and the net mouth dimensions ( $75 \times 75$  cm) were used to estimate the volume of water filtered during each tow.

The small plastic fragments collected in the nets were taken to the laboratory to extract them from the seawater samples. Polymer types of material were identified using a Fourier transform infrared spectrophotometer when fragments were too small to be distinguished visually from biological matter. In extracting small plastic fragments, the samples were not subjected to oxidative cleaning (e.g., using 30%  $H_2O_2$ ; Nuelle et al., 2014; Zhao et al., 2014) to avoid extracting fragments inside marine organisms, because our modeled results were intended for comparison with small plastic fragments carried directly by ocean currents. The numbers of extracted plastic fragments were divided by the water volumes measured by the flowmeters at each sampling station to convert them to numbers per unit seawater volume (hereinafter, “concentration” with units of pieces  $m^{-3}$ ). The observation stations in both 2014 and 2015 in the model domain are shown later in Fig. 4.

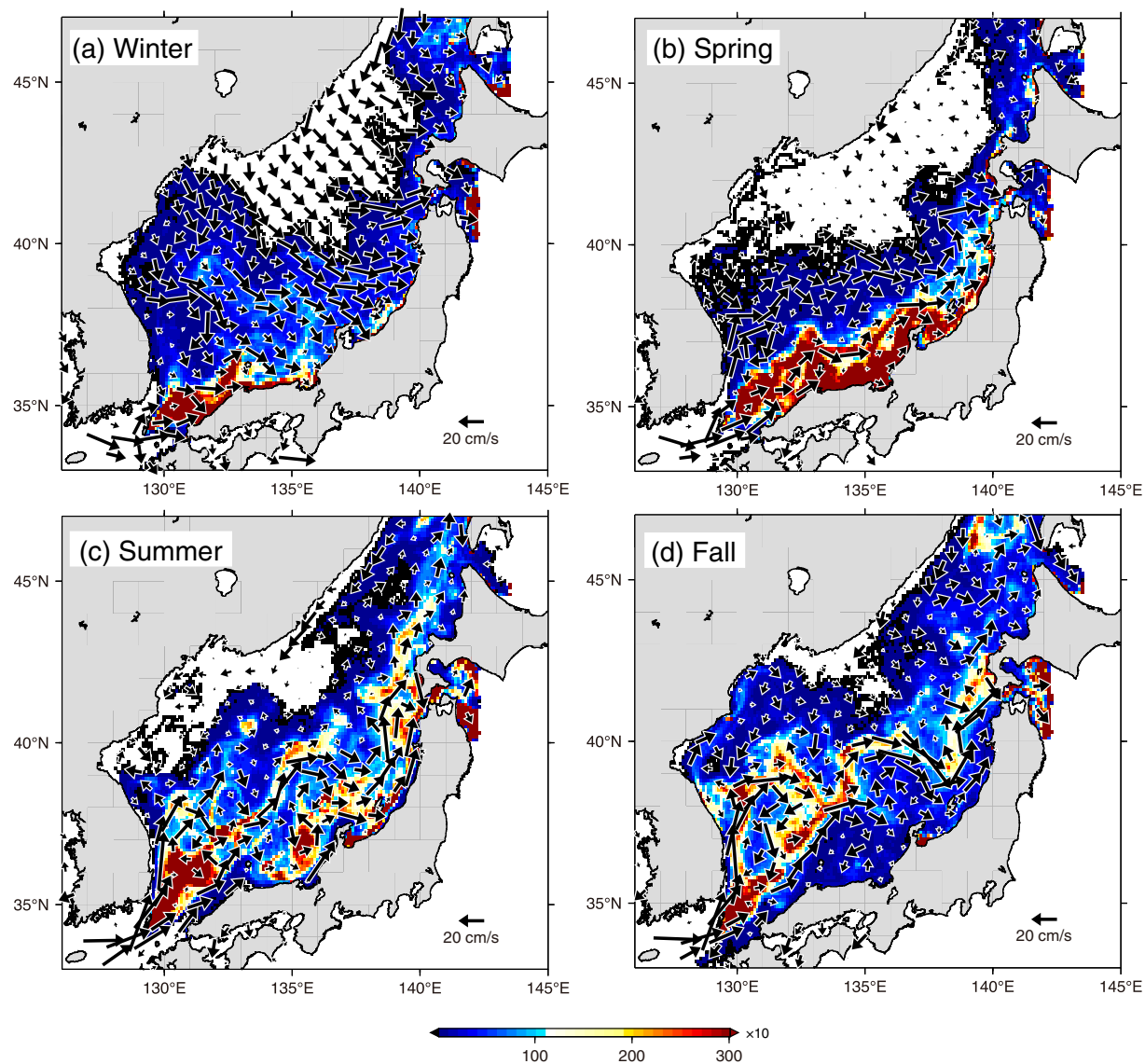


**Fig. 3.** Seasonal maps of modeled particle numbers (color shading) and surface currents (vectors) over the Sea of Japan during (a) boreal winter (December–February), (b) spring (March–May), (c) summer (June–August), and (d) fall (September–November). Modeled particle numbers with sizes from 0.3 to 10.0 mm within each 0.1° grid are integrated temporally at each season from the beginning of year 2 to the end of year 10 in the first PTM experiment. Values of color shading are indicated by the scale ( $\times 10$ ) at the bottom of the panel. Vectors represent the seasonal average of the DREAMS currents with Stokes drift at the depth of 0 m during 2014. Current vectors are scaled as indicated in the lower right corner of each panel. (For interpretation of the references to color in this figure legend, the reader is referred to the web version of this article.)

### 3. Results

#### 3.1. Seasonal variability of small plastic fragments

The particle numbers integrated spatially over the modeled Sea of Japan showed stable seasonal variation. Of note, the temporal variation of the integrated number suggests that an equilibrium state was mostly accomplished after year 2 in the first PTM experiment (Fig. 2a). Therefore, the present study analyzed the modeled outputs from the beginning of year 2 to the end of year 10 (i.e., nine years in total). The numbers of modeled particles showed a rapid increase (decrease) from January (May) to May (August) (Fig. 2b).

It was found that the spatial distributions of modeled particles in the first PTM experiment also showed remarkable seasonality within the study area (Fig. 3). During winter, when southeastward surface currents prevail over the Sea of Japan, modeled particles accumulated close to the Japanese coast in the southern part of the sea (Fig. 3a). The aforementioned increase in the numbers of modeled particles in January was consistent with this accumulation in the southern Sea of

Japan. In the subsequent spring, the accumulation of particles extended northeastward along the Japanese coast, reflecting the effect of the predominant northeastward nearshore branch of the Tsushima Current (Hase et al., 1999) (Fig. 3b). Thereafter, the areas of accumulation of the modeled particles moved offshore in summer and fall, likely becoming trapped around the subpolar front along which intense surface currents are observed (Fig. 3c and d).

#### 3.2. Model validation

In comparing the distributions of small plastic fragments based on the field surveys with the results of the first PTM experiment, the “mesoplastic ratio” is defined as  $N_{5-10 \text{ mm}} / (N_{0.3-10 \text{ mm}}) \times 100\%$ , where  $N_{5-10 \text{ mm}}$  ( $N_{0.3-10 \text{ mm}}$ ) denotes the “concentration (particle count per unit seawater volume)” of fragments with sizes from 5.0 to 10.0 mm (from 0.3 to 10.0 mm; i.e., all particles). Stations with high concentrations of microplastics with sizes  $< 5.0 \text{ mm}$  were found in northern areas (i.e., north of 39°N) in addition to the high concentrations in the Tsushima Strait (Fig. 4a). Of particular interest is the reduction in the

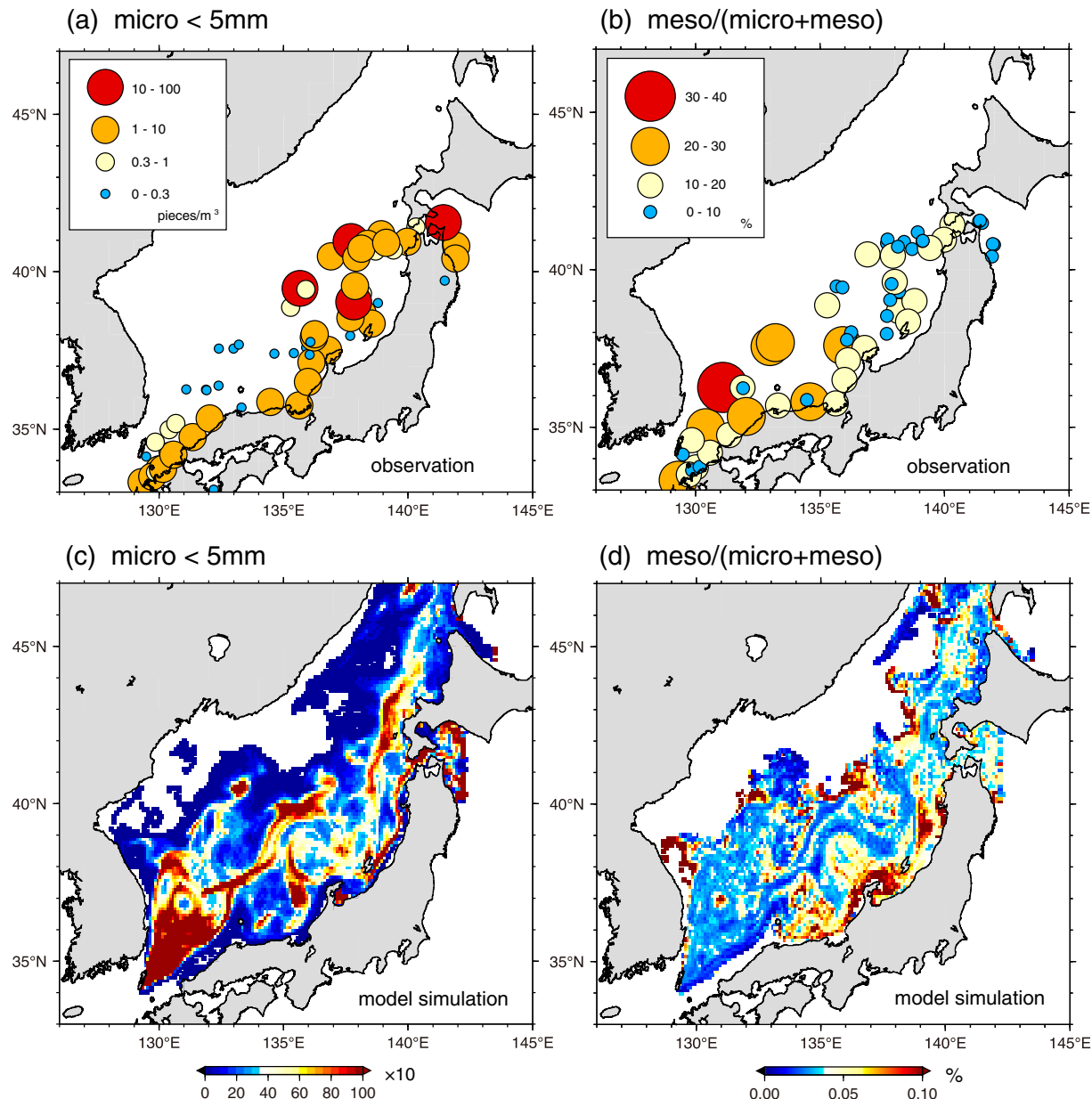


**Fig. 4.** Spatial distributions of small plastic fragments (modeled particles) based on observations (simulations) during July–August in the Sea of Japan. Panel (a) (panel (c)) denotes the concentration of microplastics at stations (numbers of microsized modeled particles within 0.1° grid). Panel (b) (panel (d)) represents the mesoplastics (mesosized modeled particle) ratio, as defined in the text. Numbers of modeled particles are integrated over the upper 1-m layer (as in the field surveys), and integrated over the period July–August from year 2 to year 10 in the first PTM experiment. In panels (c) and (d), areas without color indicate the absence of modeled particles. For comparison between panels (b) and (d), it was assumed that spherical plastic fragments degraded into smaller fragments to preserve their volumes. Thus, particle numbers in the model were converted to  $(\delta_{10} \text{ mm} / \delta)^3 \times N_8$ , where  $N_8$  denotes the numbers of particles with size  $\delta$  (10.0-mm particles are used for reference); otherwise, smaller particles released with the same abundance would be underestimated in computing the mesosized particle ratios. Scales are shown at the bottom of each lower panel (c, d). (For interpretation of the references to color in this figure legend, the reader is referred to the web version of this article.)

mesoplastic ratio in northern areas with high concentrations of microplastics (Fig. 4b). Instead, the ratio becomes large only in areas south of 39°N, especially along the Japanese coast (Fig. 4b).

The modeled particle distribution was consistent with that based on observations. The lower panels of Fig. 4 are the same as the upper panels but for the numbers of modeled particles at each grid cell. The numbers were integrated over July and August when the field surveys shown in the upper panels were mostly conducted. Note, for consistency with the survey data obtained using Neuston nets, the number of modeled particles in each grid cell was integrated over depths of 0–1 m rather than 0–5 m, as in Fig. 3. As in the observed distribution of microplastics, areas with high concentrations were found in the Tsushima Strait and areas north of 39°N (Fig. 4c). The high concentra-

tions in northern areas showed a banded structure along the region of intense surface currents (i.e., the subpolar front with surface convergence; Fig. 3c). However, the mesoplastic ratios in these northern areas were small, as in the observed ratios (Fig. 4d). In addition to the sporadic large ratios revealed in northern and western parts of the Sea of Japan, where observations were not conducted, areas with large mesoplastic ratios were found along the Japanese coast. High mesoplastic ratios were also found along the Japanese coast irrespective of season (not shown).

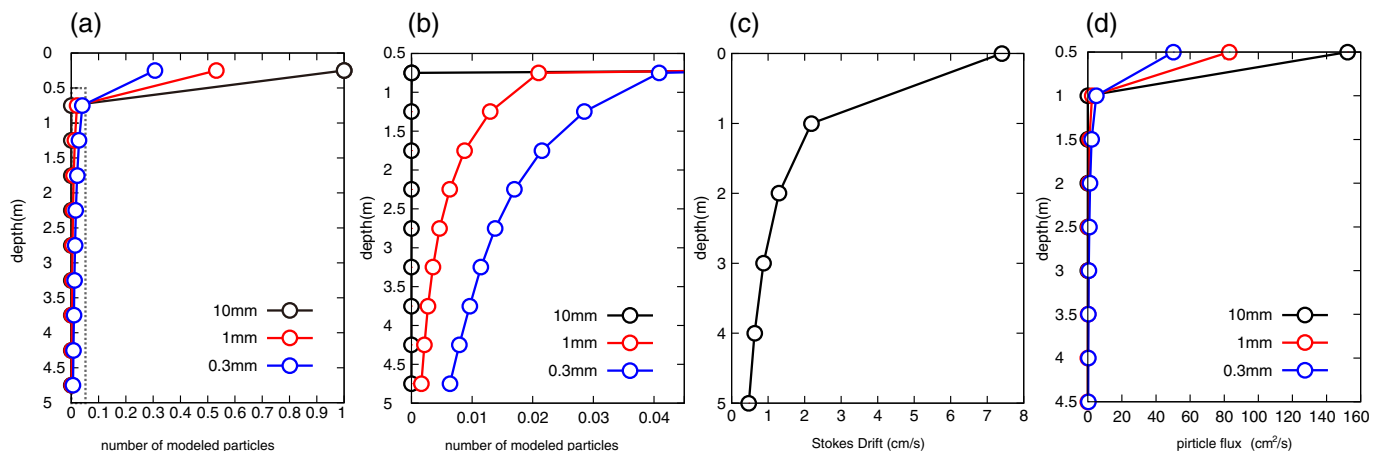


**Fig. 5.** Vertical distributions of (a, b) modeled particle numbers, (c) Stokes drift, and (d) particle flux over the Sea of Japan ( $35^{\circ}$ – $45^{\circ}$ N,  $130^{\circ}$ – $140^{\circ}$ E). (a) Vertical distribution of particle numbers integrated spatially over the Sea of Japan, and temporally over the period from the beginning of year 2 to the end of year 10. Different colored lines are used for different particle sizes, as shown in the lower right corner. Values are normalized based on values with size of 10.0 mm at depths of 0.0–0.5 m in panel (a). (b) Same as panel (a) but for enlarged graphs within the box shown in panel (a). (c) 0.25°-gridded UMWMD-derived Stokes drift averaged over the Sea of Japan ( $35^{\circ}$ – $45^{\circ}$ N,  $130^{\circ}$ – $140^{\circ}$ E) during 2014, regardless of current direction. (d) Particle flux defined as (a) particle number  $\times$  (c) Stokes drift integrated downward from the sea surface with 50-cm vertical bins. In this estimation, Stokes drift is interpolated linearly at the depth of particle numbers. (For interpretation of the references to color in this figure legend, the reader is referred to the web version of this article.)

## 4. Discussion

### 4.1. Transport processes of micro- and mesoplastics

It is considered that the contribution of Stokes drift to particle motion differs depending on particle size. Generally, lighter small plastic fragments are more likely than heavier particles to remain in the uppermost ocean layer because of the buoyancy force exerted on them (Reisser et al., 2015). The first PTM experiment successfully reproduced the situation in which the modeled particles remained confined within the upper 5-m layer, as observed by Reisser et al. (2015) (Fig. 5a and b). The buoyancy force acting against friction exerted on small plastic fragments decreases as their sizes decrease. Thus, the smaller the modeled particles become, the deeper they drift within the upper ocean layer with turbulent mixing (Eqs. (4) and (5), and Fig. 5b). However, Stokes drift in the upper layer is always faster than in deeper layers (Fig. 5c); thus, buoyant large particles drifting in the uppermost layer are likely to move more rapidly than smaller particles in terms of Stokes drift. In fact, the magnitude of the modeled “particle flux (particle number  $\times$  Stokes drift integrated over 50-cm vertical bins from the sea surface)” of 10.0-mm-sized particles is approximately three times greater than that of 0.3-mm particles at the depth of 0.5 m (Fig. 5d). However, it should be noted that particle fluxes are concentrated mostly above the depth of 1 m, irrespective of particle size, because of the combination of surface-accumulated particle numbers (Fig. 5a and b) and Stokes drift (Fig. 5c).

The predominance of mesoplastics in the southern part of the Sea of Japan and along the Japanese coast (Fig. 4b and d) results from the abovementioned size dependency of particle motion in terms of the Stokes drift. This was demonstrated clearly by the second PTM experiment, which provided a comparison between horizontal two-dimensional PTMs (i.e., second PTM) with and without the Stokes drift at 0-m depth (i.e., the fastest drift). These experiments were likely to amplify the difference in motion between particles beneath (less buoyant) and within (buoyant) the layers where Stokes drift prevails ( $< 5$  m; see Fig. 5c). The modeled particles in the second PTM without Stokes drift showed a banded structure with a high concentration extending from the Tsushima Strait to areas north of the Sea of Japan during summer (July–August) (Fig. 6a), which is consistent with the distribution of micro-sized particles (Fig. 4c). It is therefore suggested that Stokes drift is not critical in the motion of less buoyant micro-sized particles (hence, microplastics in nature) moving in deeper layers

(Fig. 5b). The modeled particles in the second PTM with Stokes drift during summer showed the banded structure is frequently interrupted (Fig. 6b), and that the ratio of particles in the second PTM with Stokes drift (Fig. 6b) to the sum of Fig. 6a and b becomes large along the Japanese coast (Fig. 6c). It is noted that the appearance of these high ratios along the Japanese coast (Fig. 6c) is similar to that of the observed (Fig. 4b) and modeled (Fig. 4d) mesoplastic ratios.

The predominance of mesosized particles (hence, mesoplastics) along the Japanese coast (Figs. 4b, d, and 6c) can be explained by the fact that the southeastward currents, prevailing only in winter (Fig. 3a), result from Stokes drift (Fig. 7). In winter, buoyant larger particles are likely to be carried southeastward to the Japanese coast because of the intensified Stokes drift within the surface layer (Fig. 7b), whereas smaller particles drifting in the deeper layer will be carried toward the Tsugaru Strait (a northern exit of the Sea of Japan) by northeastward ocean currents (Fig. 7a). It is therefore reasonable that modeled particles become abundant within the Sea of Japan, especially during winter, as particle sizes increase in the first PTM experiment (Fig. 8a). If modeled particles were released from sources other than the Tsushima Strait, from which the particles were immediately carried into the Sea of Japan by ocean currents (Fig. 3), the relatively large mesosized particles would be more abundant along the Japanese coast than shown in Fig. 4(d). This is because the buoyant mesoplastics that originate from urban centers and shipping traffic around the Japanese coasts might be trapped close to the coast by the southeastward Stokes drift during winter. If this were the case, the small abundance of mesosized particles in the area close to the Tsushima Strait (south of  $37^{\circ}$ N, and west of  $132^{\circ}$ E; Fig. 4d) would increase, as found in the observations (Fig. 4b). In addition, it is suggested that Stokes drift carries less buoyant polypropylene fragments ( $0.85$ – $0.9$  g cm $^{-3}$ ; Andrade, 2003) more rapidly than polyethylene fragments ( $0.91$ – $0.97$  g cm $^{-3}$ ), although the effects of polymer type were neglected in both the present PTM and the field surveys.

The numbers of modeled particles decrease rapidly within the study area from May to August irrespective of size (Figs. 2 and 8). This is because the nearshore branch of the Tsushima Current, which flows northeastward along the Japanese coast (Hase et al., 1999), carries the modeled particles along the Japanese coast toward the open ocean via the Tsugaru Strait (Fig. 9). In addition, the modeled particles also flow out toward the North Pacific via the Soya Strait, although the number of particles passing through this strait is smaller than through the Tsugaru Strait over the computation period (not shown).

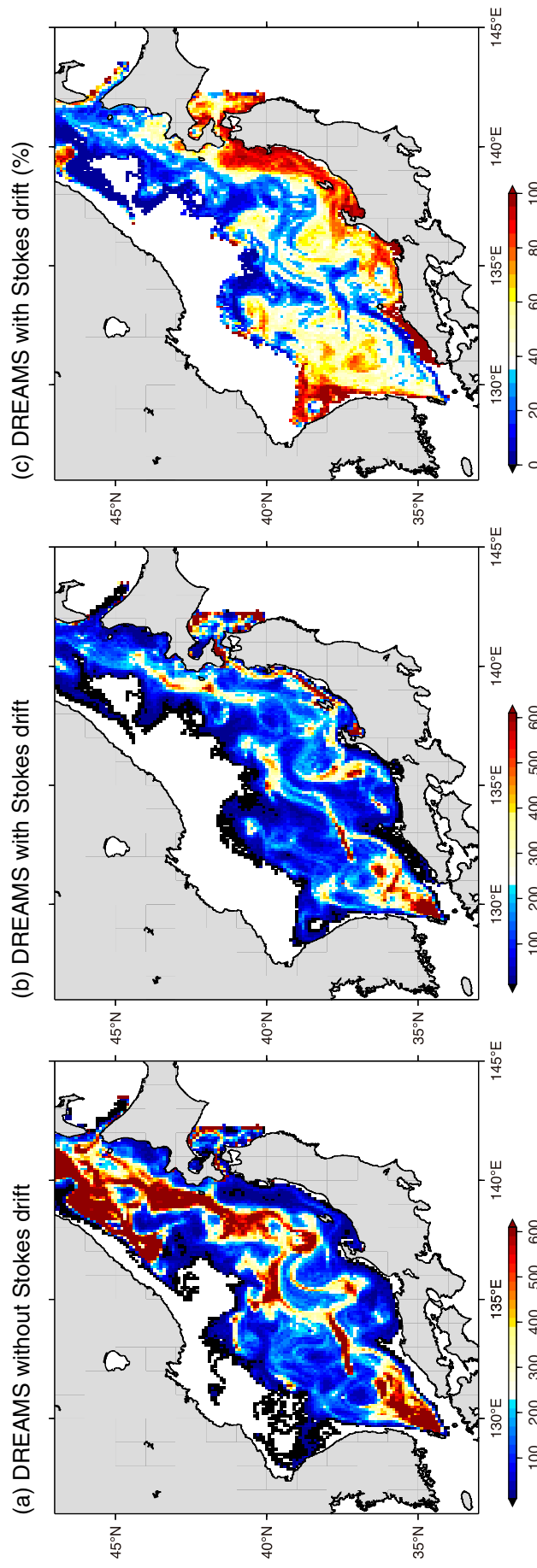


**Fig. 6.** Maps of particle numbers integrated at each  $0.1^{\circ}$  grid in the second PTM experiment. Panels (a) and (b) are PTMs using the DREAMS currents without and with the surface Stokes drift (i.e., drift at 0-m depth), respectively. Numbers are integrated over the period July–August from year 2 to year 10. Panel (c) denotes the ratio of modeled particle numbers computed using the DREAMS currents with Stokes drift at 0-m depth, the ratio is computed as  $N_D + s / (N_D + N_s + s) \times 100\%$ , where  $N_D$  ( $N_s$ ) denotes the numbers of modeled particles computed from the DREAMS currents with (without) the surface Stokes drift. Values are represented by color shading, as shown in the scale at the bottom of each panel. (For interpretation of the references to color in this figure legend, the reader is referred to the web version of this article.)

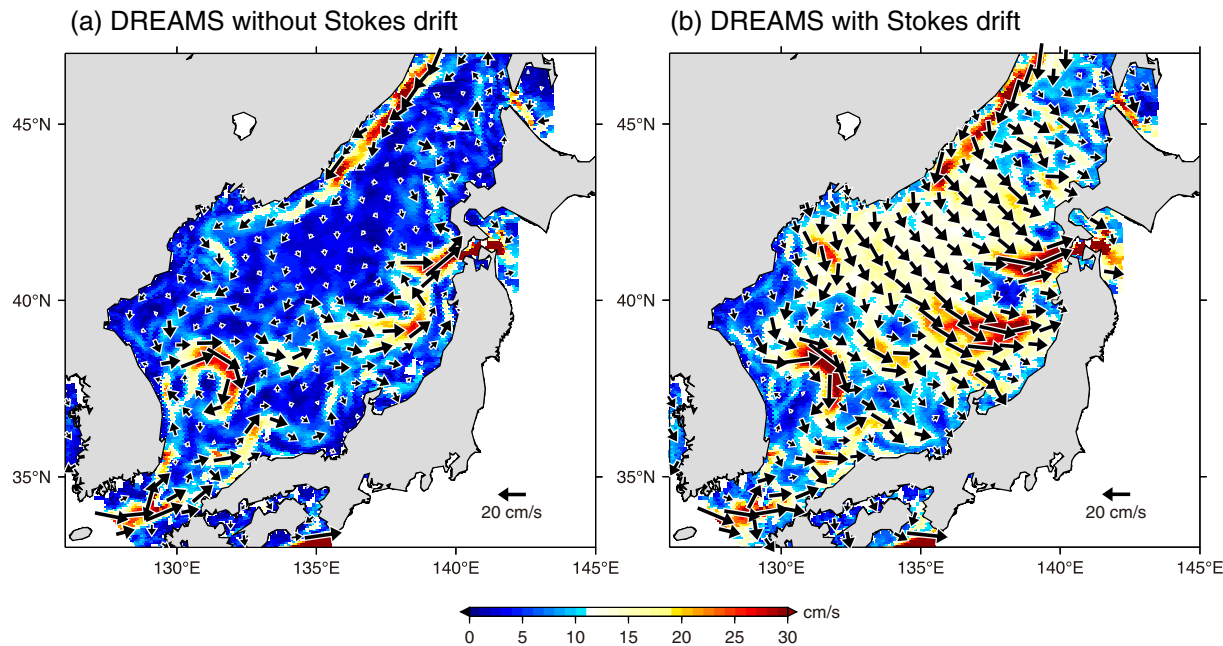


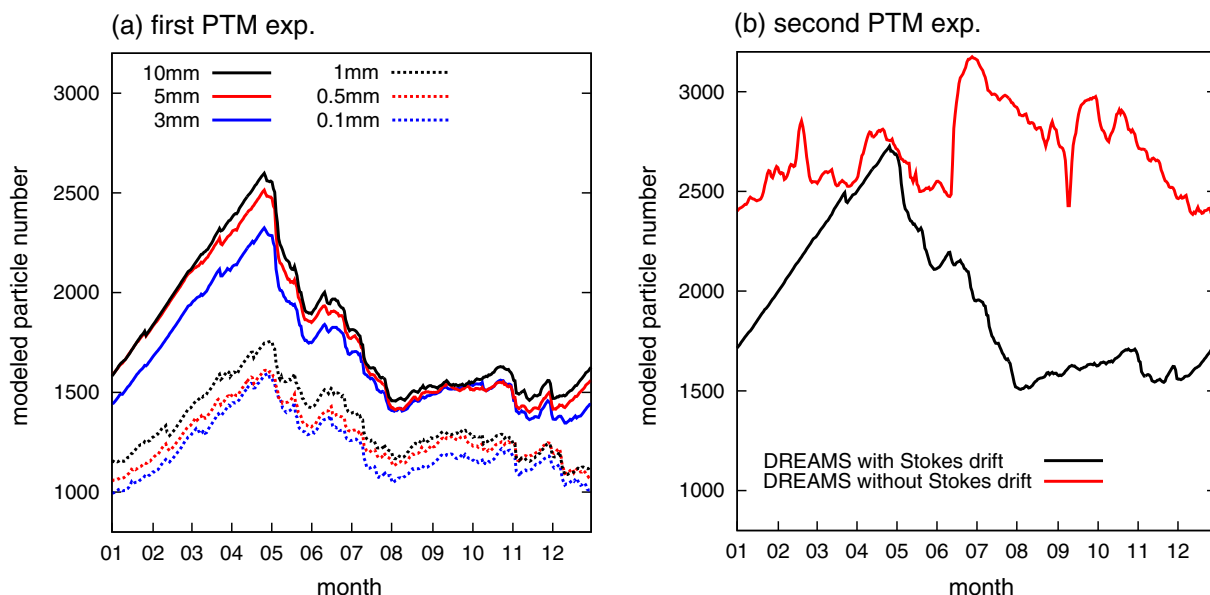
**Fig. 7.** Surface current vectors (arrows) and speeds (color shading) averaged over winter (December–February) 2014 in the Sea of Japan for the DREAMS currents (a) without and (b) with Stokes drift at 0-m depth. Current vectors are scaled as shown in the lower right corner of each panel. Current speed scale is shown at the bottom of the panels. (For interpretation of the references to color in this figure legend, the reader is referred to the web version of this article.)

#### 4.2. Average transit time of small plastic fragments

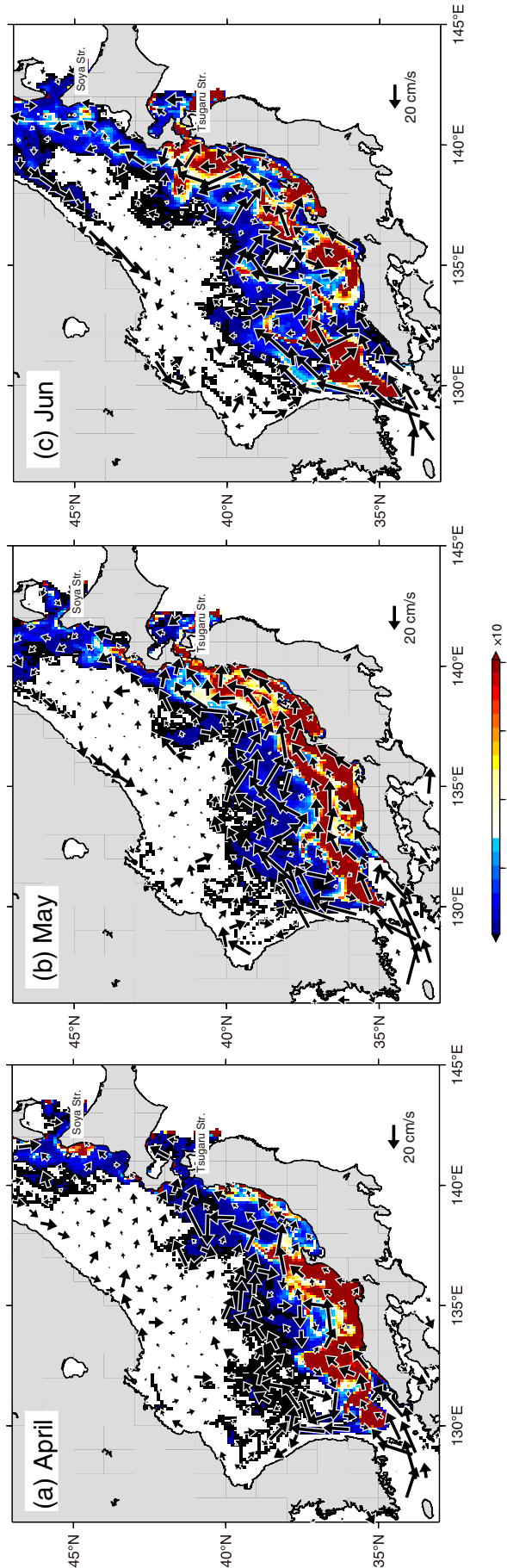
Computing the average transit time revealed the critical role of Stokes drift in the movement of small plastic fragments. In the first PTM experiment, where particles with different sizes were released, it was found that the abundance of larger particles became greater than smaller particles throughout the year (Fig. 8a). This meant that the average transit time of larger particles was longer than smaller particles. In fact, the averaged transit times of particles with sizes of 0.3 and 10.0 mm varied from 122 to 182 days, respectively (Table 1). This is reasonable because the southeastward Stokes drift selectively carried mesosized particles (hence, mesoplastics) toward the Japanese

coast (Fig. 4b and d), along which the northeastward ocean currents were weaker than along the subpolar front (Fig. 7a). In reality, small plastic fragments drifting close to the coast are likely to wash ashore, where degradation occurs due to exposure to ultraviolet radiation and mechanical erosion. It is therefore considered that degradation of mesoplastics to microplastics is enhanced in the Sea of Japan where mesoplastics drift near the coast for long periods.

Unless Stokes drift carries the fragments to the south of the subpolar front, the average transit time of small plastic fragments increases because they become trapped within the cyclonic gyre to the north of the front (Fig. 7a). It was found that the seasonality of particle numbers almost disappears in the second PTM experiment without Stokes drift



**Fig. 8.** Same as Fig. 2b but for each particle size (a) and the second PTM experiment (b). As shown in the upper portion, different line colors and types are used for different particle sizes of 10.0, 5.0, 3.0, 1.0, 0.5, and 0.3 mm. Solid black (red) curve in panel (b) indicates the number of the modeled particles computed using the DREAMS currents with (without) Stokes drift at 0-m depth. (For interpretation of the references to color in this figure legend, the reader is referred to the web version of this article.)

**Table 1**

Average transit times (days) of modeled particles passing through the Sea of Japan according to particle size (first six columns) and second PTM experiment (final two columns). Average transit time is computed as  $N / R$ , where  $N$  denotes the modeled particle numbers integrated spatially over the Sea of Japan ( $35^{\circ}$ – $45^{\circ}$ N,  $130^{\circ}$ – $140^{\circ}$ E) and averaged temporally over the period from the beginning of year 10 to the end of year 10 (Fig. 8), and  $R$  denotes the supply rate of particles into the model domain (i.e., 10 modeled particles released once daily at a single point in the Tsushima Strait).

0.3 mm	0.5 mm	1 mm	3 mm	5 mm	10 mm	DREAMS + Stokes	DREAMS
122	128	135	168	177	182	194	270

(Fig. 8b). This is because a rapid decrease of particle numbers occurs from May to August (Figs. 2 and 8), which can be attributed to the influence of the nearshore branch of the Tsushima Current along the Japanese coast (Fig. 9). The average transit time was estimated at 194 days for particles carried by the DREAMS currents with Stokes drift at the depth of 0 m, whereas the average transit time of particles carried by the DREAMS currents alone was 270 days (Table 1).

#### 4.3. Improvement points of the model

It should be noted that the model presented here is immature in reflecting the understanding of the fate of small plastic fragments (hence, their transit time) in the ocean. In fact, it was found that the spatial correlation between the ratio of observed and modeled mesoplastics in the Sea of Japan was not significant, especially around the Tsushima Strait (Fig. 4b and d). In addition to the source(s) of the small plastic fragments, consideration of the following five points might improve model accuracy. First, the exchange processes of small plastic fragments between beaches and surf zones should be incorporated realistically in the PTMs. In the present model, a particle carried into a land cell was returned immediately to the oceanic cell in which it was located at the previous computational time step. However, the time required for re-drifting to the oceanic domain should be given to the model according to the timescale over which small plastic fragments actually remain on the beaches. Thereby, the average transit time of mesoplastics in the Sea of Japan might be longer than the present estimates, because mesoplastics abundant in areas close to the coast are likely to wash ashore in the actual ocean. In addition to the re-drifting process, the behavior of small plastic fragments in surf zones, unresolved in the present model, should be incorporated as part of the process of small plastic fragments being washed ashore. Second, the degradation of mesoplastics to microplastics on beaches must be reproduced in the model (Critchell and Lambrechts, 2016) when PTMs are used to reproduce the long-term transport required for degradation. Third, as well as Stokes drift, ocean currents with high vertical resolution in the uppermost layer might be required to reproduce the motion of buoyant small plastic fragments more accurately. In the present application, however, the DREAMS currents at 4-m depth were used in the three-dimensional PTM regardless of the particle depths. In addition to the above three physical processes, as reviewed by Hardesty et al. (2017), ingestion by marine organisms (e.g., Browne et al., 2008; Boerger et al., 2010; Murray and Cowie, 2011; Cole et al., 2015; Desforges et al., 2015) and settling by biofouling (Long et al., 2015) might be nonnegligible sink terms in the PTMs. However, it is difficult currently to incorporate all the above processes into PTMs because the pathways of small plastic fragments remain ambiguous in the actual ocean.

#### 5. Conclusions

The schematic in Fig. 10 summarizes the transport processes of small plastic fragments in the Sea of Japan. In the present study, it was

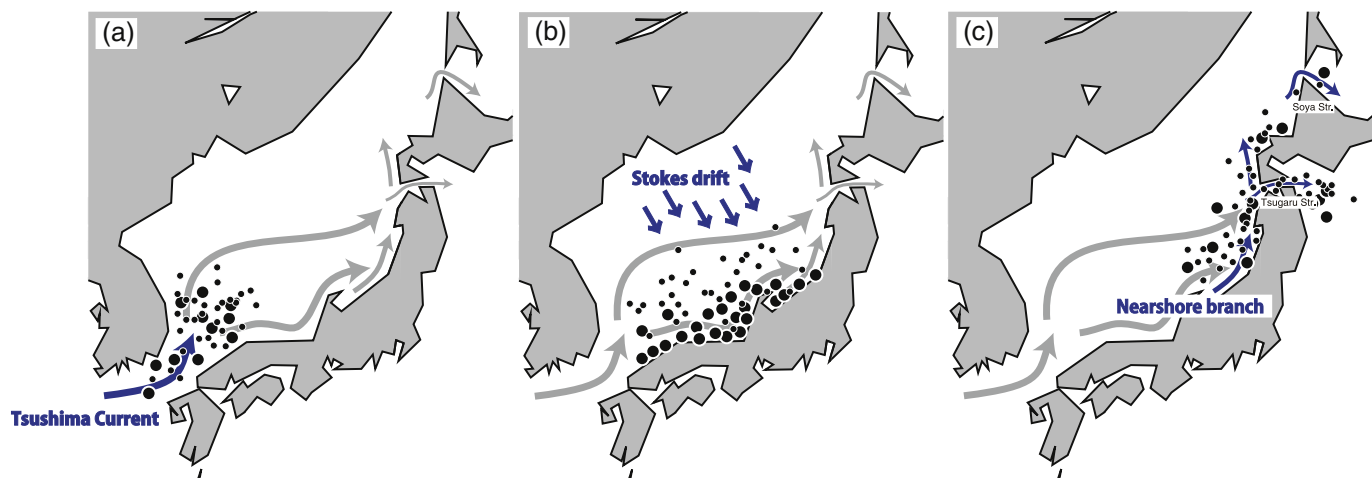


**Fig. 10.** Schematic of the transport processes of mesoplastics (large dots) and microplastics (small dots) in the Sea of Japan. Gray arrows show warm ocean currents from south to north throughout the year. Mesoplastics and microplastics are carried by (a) the Tsushima Current, (b) in conjunction with Stokes drift, especially in winter, and (c) the nearshore branch of the Tsushima Current (see blue arrows for the processes in each panel). (For interpretation of the references to color in this figure legend, the reader is referred to the web version of this article.)

assumed that small plastic fragments were mostly carried by the northeastward Tsushima Current from the East China Sea via the Tsushima Strait (Fig. 10a) because of the large amount of mismanaged plastic waste generated in China and Southeast Asian countries (Jambeck et al., 2015). The southeastward Stokes drift prevailing during winter (Fig. 7) carries the plastic fragments toward the Japanese coast (Fig. 10b). Thereby, relatively large mesosized plastic fragments accumulate along the Japanese coast more rapidly than microsized plastic particles because particle flux becomes larger as particle size increase (Figs. 5d and 10b). Thus, Stokes drift has a role in selectively transporting mesoplastics close to the Japanese coast along which the average transit time is extended because of the presence of relatively weak ocean currents. In reality, mesoplastics drifting close to the coast are likely to wash ashore and degrade to microplastics. The plastic fragments along the Japanese coast are carried northeastward by the nearshore branch of the Tsushima Current to the open ocean via the Tsugaru and Soya straits (Fig. 10c).

The above scenario suggests that the southeastward Stokes drift in winter has the secondary role of discharging plastic fragments efficiently both from the cyclonic gyre to the north of the subpolar front and from the Sea of Japan. Despite Stokes drift prevailing in the uppermost ocean layer in winter, it might appear paradoxical to find that the abundance (total particle count) of microplastics in the East Asian seas, including the Sea of Japan, is one order of magnitude larger than in the North Pacific and the world oceans (Isobe et al., 2015). One plausible reason for this abundance of microplastics is that the volume of mismanaged plastic waste discharged into the East Asian seas is the largest in the world (Jambeck et al., 2015).

## Acknowledgments

The authors would like to thank Prof. Hidenori Aiki (Nagoya University) and Prof. Mark Donelan (University of Miami) for their helpful comments on the wave model. Thanks are also extended to the Captains, officers, and crews of the *T/V Umitaka-maru* and *T/V Shinyo-maru* for their assistance during the field surveys. Part of this research was supported by the Ministry of the Environment, Japan, JANUS, Naigai Map Production, and the Environmental Research and Technology Development Fund (4-1502) of the Ministry of the Environment. Two reviewers provided valuable comments that helped us improve this paper significantly.

## References

- Andrady, A., 2003. Common plastics materials. In: Andrady, A.L. (Ed.), *Plastics and the Environment*. John Wiley and Sons Inc., New Jersey, USA, pp. 77–121.
- Andrady, A.L., 2011. Microplastics in the marine environment. *Mar. Pollut. Bull.* 62, 1596–1605.
- Borger, C.M., Lattin, G.L., Moore, S.L., Moore, C.J., 2010. Plastic ingestion by planktivorous fishes in the North Pacific Central Gyre. *Mar. Pollut. Bull.* 60, 2275–2278.
- Bonjean, F., Lagerloef, G.S.E., 2002. Diagnostic model and analysis of the surface currents in the tropical Pacific Ocean. *J. Phys. Oceanogr.* 32, 2938–2954.
- Browne, M.A., Dissanayake, A., Galloway, T.S., Lowe, D.M., Thompson, R.C., 2008. Ingested microscopic plastic translocates to the circulatory system of the mussel, *Mytilus edulis* (L.). *Environ. Sci. Technol.* 42, 5026–5031. <http://dx.doi.org/10.1021/es800249a>.
- Chassignet, E.P., Hurlburt, H.E., Smedstad, O.M., Halliwell, G.R., Hogan, P.J., Walcroft, A.J., Baraille, R., Bleck, R., 2007. The HYCOM (Hybrid Coordinate Ocean Model) data assimilative system. *J. Mar. Sys.* 65, 60–83.
- Cole, M., Lindeque, P., Halsband, C., Galloway, T.S., 2011. Microplastics as contaminants in the marine environment: a review. *Mar. Pollut. Bull.* 62, 2588–2597.
- Cole, M., Lindeque, P., Fileman, E., Halsband, C., Galloway, T.S., 2015. The impact of polystyrene microplastics on feeding, function and fecundity in the marine copepod *Calanus helgolandicus*. *Environ. Sci. Technol.* 49, 1130–1137.
- Cózar, A., Echevarría, F., González-Gordillo, J.I., Irigoien, X., Úbeda, B., Hernández-León, S., Palma, Á.T., Navarro, S., García-de-Lomas, J., Fernández-de-Puelles, M.L., Duarte, C.M., 2014. Plastic debris in the open ocean. *Proc. Natl. Acad. Sci.* 111, 10239–10244.
- Critchell, K., Lambrechts, L., 2016. Modelling accumulation of marine plastics in the coastal zone; what are the dominant physical processes? *Estuar. Coast. Shelf Sci.* 171, 111–122.
- Desforges, J.-P., Galbraith, M., Ross, P.S., 2015. Ingestion of microplastics by zooplankton in the northeast Pacific Ocean. *Arch. Environ. Contam. Toxicol.* <http://dx.doi.org/10.1007/s00244-015-0172-5>.
- Donelan, M.A., Curcic, M., Chen, S.S., Magnusson, A.F., 2012. Modeling waves and wind stress. *J. Geophys. Res.* 117, C00J23. <http://dx.doi.org/10.1029/2011JC007787>.
- Enders, K., Lenz, R., Stedman, C.A., Nielsen, T.G., 2015. Abundance, size and polymer composition of marine microplastics > 10 mm in the Atlantic Ocean and their modeled vertical distribution. *Mar. Pollut. Bull.* 100, 70–81.
- Eriksen, M., Lebreton, L.C.M., Carson, H.S., Theil, M., Moore, C.J., Borerro, J.C., Galgani, F., Ryan, P.G., Reisser, J., 2014. Plastic pollution in the world's oceans: more than 5 trillion plastic pieces weighing over 250,000 tons afloat at sea. *PLoS One* 9 (12), e111913. <http://dx.doi.org/10.1371/journal.pone.0111913>.
- Gregory, M.R., 1996. Plastic 'scrubbers' in hand cleansers: a further (and minor) source for marine pollution identified. *Mar. Pollut. Bull.* 32, 867–871.
- Hardesty, B.D., Harai, J., Isobe, A., Lebreton, L., Maximenko, N., Potemra, J., van Sebille, E., Vethaak, A.D., Wilcox, C., 2017. Using numerical model simulations to improve the understanding of micro-plastic distribution and pathways in the Marine Environment. *Front. Mar. Sci.* 4 (30). <http://dx.doi.org/10.3389/fmars.2017.00030>.
- Hase, H., Yoon, J.-H., Kotera, W., 1999. The current structure of the Tsushima Warm Current along the Japanese coast. *J. Oceanogr.* 55, 217–235.
- Hirose, N., 2011. Inverse estimation of empirical parameters used in a regional ocean circulation model. *J. Oceanogr.* 67, 323–336.
- Hirose, N., Takayama, K., Moon, J.-H., Watanabe, T., Nishida, Y., 2013. Regional data assimilation system extended to the East Asian marginal seas. *Umi to Sora [Sea and Sky]* 89, 43–51.
- Isobe, A., Kako, S., Chang, P.-H., Matsuno, T., 2009. Two-way particle tracking model for

- specifying sources of drifting objects: application to the East China Sea shelf. *J. Atmos. Ocean. Technol.* 26, 1672–1682.
- Isobe, A., Kubo, K., Tamura, Y., Kako, S., Nakashima, E., Fujii, N., 2014. Selective transport of microplastics and mesoplastics by drifting in coastal waters. *Mar. Pollut. Bull.* 89, 324–330.
- Isobe, A., Tokai, T., Uchida, K., Iwasaki, S., 2015. East Asian seas, a hot spot of pelagic microplastics. *Mar. Pollut. Bull.* 101, 618–623.
- Isobe, A., Uchiyama-Matsumoto, K., Uchida, K., Tokai, T., 2017. Microplastics in the Southern Ocean. *Mar. Pollut. Bull.* 114, 623–626.
- Jambeck, J.R., Geyer, R., Wilcox, C., Siegler, T.R., Perryman, M., Andrade, A., Narayan, R., Law, K.L., 2015. Plastic waste inputs from land into the ocean. *Science* 347, 768–771.
- Kako, S., Isobe, A., Kubota, M., 2011. High-resolution ASCAT wind vector dataset gridded by applying an optimum interpolation method in the global ocean. *J. Geophys. Res.-Atmos.* 116, D23107. <http://dx.doi.org/10.1029/2010JD015484>.
- Kako, S., Isobe, A., Kataoka, T., Hinata, H., 2014. A decadal prediction of the quantity of plastic marine debris littered on beaches of the East Asian marginal seas. *Mar. Pollut. Bull.* 81, 174–184.
- Kubota, M., 1994. A mechanism for the accumulation of floating marine debris north of Hawaii. *J. Phys. Oceanogr.* 24, 1059–1064.
- Kukulka, T., Proskurowski, G., Moret-Ferguson, S., Meyer, D.W., Law, K.L., 2012. The effect of wind mixing on the vertical distribution of buoyant plastic debris. *Geophys. Res. Lett.* 39, L07601. <http://dx.doi.org/10.1029/2012GL051116>.
- Long, M., Moriceau, B., Gallinari, M., Lambert, C., Huvet, A., Raffray, J., Soundant, P., 2015. Interactions between microplastics and phytoplankton aggregates: impact on their respective fates. *Mar. Chem.* 175, 39–46.
- Maximenko, N., Hafner, J., Niiler, P., 2012. Pathways of marine debris from trajectories of Lagrangian drifters. *Mar. Pollut. Bull.* 65, 51–62.
- Miyazawa, Y., Zhang, R., Guo, X., Tamura, H., Ambe, D., Lee, J.S., Okuno, A., Yoshinari, H., Setou, T., Komatsu, H., 2009. Water mass variability in the western North Pacific detected in a 15-year eddy resolving ocean reanalysis. *J. Oceanogr.* 65, 737–756.
- Murray, F., Cowie, R.P., 2011. Plastic contamination in the decapod crustacean *Nephrops norvegicus* (Linnaeus, 1758). *Mar. Pollut. Bull.* 62, 1207–1217.
- Nuelle, M.-T., Dekiff, J.H., Remy, D., Fries, E., 2014. A new analytical approach for monitoring microplastics in marine sediments. *Environ. Pollut.* 184, 161–169.
- Proctor, R., Flather, R.A., Elliott, A.J., 1994. Modelling tides and surface drift in the Arabian Gulf—application to the Gulf oil spill. *Cont. Shelf Res.* 14, 531–545.
- Reisser, J., Slat, B., Noble, K., du Plessis, K., Epp, M., Proietti, M., de Sonneville, J., Becker, T., Pattiaratchi, C., 2015. The vertical distribution of buoyant plastics at sea: an observational study in the North Atlantic Gyre. *Biogeosciences* 12, 1249–1256.
- Richardson, P.L., 1997. Drifting in the wind: leeway error in shipdrift data. *Deep Sea Res.* 44, 1877–1903.
- Smagorinsky, J., 1963. General circulation experiments with the primitive equations: I. The basic experiment. *Mon. Weather Rev.* 91, 99–164.
- Takeoka, H., 1984. Fundamental concepts of exchange and transport time scales in a coastal sea. *Cont. Shelf Res.* 3 (3), 311–326.
- Usui, N., Ishizaki, S., Fujii, Y., Tsujino, H., Yasuda, T., Kamachi, M., 2006. Meteorological Research Institute multivariate ocean variational estimation (MOVE) system: some early results. *Adv. Space Res.* 37, 806–822. <http://dx.doi.org/10.1016/j.asr.2005.09.022>.
- Willis, J.K., Fu, L.-L., 2008. Combining altimeter and subsurface float data to estimate the time-averaged circulation in the upper ocean. *J. Geophys. Res.* 113, C12017. <http://dx.doi.org/10.1029/2007JC004690>.
- Zhao, S., Zhu, L., Wang, T., Li, D., 2014. Suspended microplastics in the surface water of the Yangtze Estuary System, China: first observations on occurrence, distribution. *Mar. Pollut. Bull.* 86, 562–568.